Journal of Volcanology and Geothermal Research 199 (2011) 177–192

Contents lists available at ScienceDirect

Journal of Volcanology and Geothermal Research

journal homepage: www.elsevier.com/locate/jvolgeores

New data on the Late Cenozoic basaltic volcanism in Syria, applied to its origin

V.G. Trifonov [a,*], A.E. Dodonov [a], E.V. Sharkov [b], D.I. Golovin [a], I.V. Chernyshev [b], V.A. Lebedev [b], T.P. Ivanova [c], D.M. Bachmanov [a], M. Rukieh [d], O. Ammar [d], H. Minini [d], A.-M. Al Kafri [d], O. Ali [d]

[a] Geological Institute of the Russian Academy of Sciences (RAS), 7 Pyzhevsky, Moscow 119017, Russia
[b] Institute of Geology of Ore Deposits, Petrography, Mineralogy and Geochemistry of the RAS, 35 Staromonetny, Moscow 119017, Russia
[c] Institute of Dynamics of Geospheres of the RAS, Block 6, 38 Leninsky Ave., Moscow 117334, Russia
[d] General Organization of Remote Sensing, P.O. Box 12586, Damascus, Syria

ARTICLE INFO

Article history:
Received 24 June 2009
Accepted 19 January 2010
Available online 29 January 2010

Keywords:
Syria
Ethiopia–Afar superplume
Arabian plate
Dead Sea transform zone
Late Cenozoic basalts
K–Ar dates
tectonics
magmatic sources

ABSTRACT

New data on geology and 21 K–Ar dates of the Late Oligocene–Quaternary basalts in Syria, combined with analysis of the new and previous data are used to reconstruct the volcanic history and relations between it and tectonic events. Volcanism began at the end of Oligocene (26–24 Ma) and was concentrated in the Late Oligocene–Early Miocene along a N-trending band, which stretches from the Jebel Arab (Harrat Ash Shaam) up to Kurd Dagh and southern Turkey. Activity waned in the Middle Miocene (17–12 Ma), but was resumed in the same band in the Tortonian and increased in the Messinian and Early Pliocene (6.3–4 Ma), when volcanism spread to the Shin Plateau and its coastal extension. After a brief hiatus ~4–3.5 Ma, volcanism became still more intensive and spread from the N-trending band to the east into the northern margin of the Mesopotamian Foredeep and to the west into the Dead Sea Transform zone. Additional eruptions continued into the Holocene.

Volcanism lasted >25 million years in the Jebel Arab Highland and >15 million years in the Aleppo Plateau. The long duration of volcanism in the same parts of the moving Arabian plate and absence of records of one-way migration of the activity mean that the magmatic sources moved together with the plate, i.e., they were situated within the lithosphere mantle. Coincidence of the tectonic and volcanic stages of the Arabian plate development proves that volcanic activity depended on the geodynamic situation, caused by the plate motion. Situated within the lithosphere, magmatic sources within this transverse band were possibly caused by thermal and deforming influences of the asthenospheric lateral flow, moved laterally from the Ethiopia–Afar deep superplume.

1. Introduction

Syria is located in the northern part of the Arabian plate along the boundary zones between it and the African (the Levantin basin of the Mediterranean) and Anatolian plates. The boundary zone between the Arabian and African plates is defined by the Levant fault zone (Dead Sea Transform, DST) and associated structures (Garfunkel and Ben-Abraham, 2001; Rukieh et al., 2005). Late Cenozoic (Late Oligocene to Quaternary) basalts cover large areas in the northern and central parts of the Arabian plate (Camp and Roobol, 1989) and occupy Syria (Geological Map of Syria, 1964; Ponikarov et al., 1967; Mouty et al., 1992; Chorowicz et al., 2004) and adjacent territories of Turkey up to the Taurus suture (Çapan et al., 1987; Yilmaz et al., 1998) and Jordan up to Saudi Arabia (Barberi et al., 1979; Ilani et al., 2001) (Fig. 1). Similar, but less extensive volcanism occurs in the DST zone (Garfunkel, 1989; Sharkov et al., 1994; Polat et al., 1997; Yürür and Chorowicz, 1998; Abdel-Rahman and Nassar, 2004; Segev, 2005).

All researchers agree that the basalts were generated in the mantle, but explain their origin by different processes. Garfunkel (1989) considered that the basalts were related to "several short-lived upwellings, which formed intermittently beneath a wide region." Stein and Hofmann (1992) considered that relative homogeneity of the basalts in terms of the Sr–Nd isotopic ratios was caused by their common source represented by a plume in the base of the Arabian lithosphere. Sobolev et al. (2005) agreed with the "plume" origin of the Arabian basalts, but argued they are linked to the Ethiopian-Afar deep mantle superplume. Ershov and Nikishin (2004) gave the same explanation. They considered that the superplume penetrated to the upper mantle from the lower mantle 45–37 Ma (Ebinger and Sleep, 1998) and formed two lateral sub-lithosphere flows: to the south (Kenya) and to the north. The second flow propagated in succession beneath the southern Arabia and Red Sea region (~28–27 Ma), beneath central and northern Arabia (13–9 Ma), the Armenian Highland (~11 Ma) and the Great Caucasus (9–7 Ma). Ershov and Nikishin referred to the seismotomographic data on existence of the "hot" (low-rate) sub-lithosphere volumes beneath these regions (Debayle et al., 2001; Ershov et al., 2001) as an evidence of the flow.

* Corresponding author. Tel.: +7 495 9539318, +7 916 5404052; fax: +7 495 9510443.
E-mail address: trifonov@ginras.ru (V.G. Trifonov).

0377-0273/$ – see front matter © 2010 Published by Elsevier B.V.
doi:10.1016/j.jvolgeores.2010.01.013

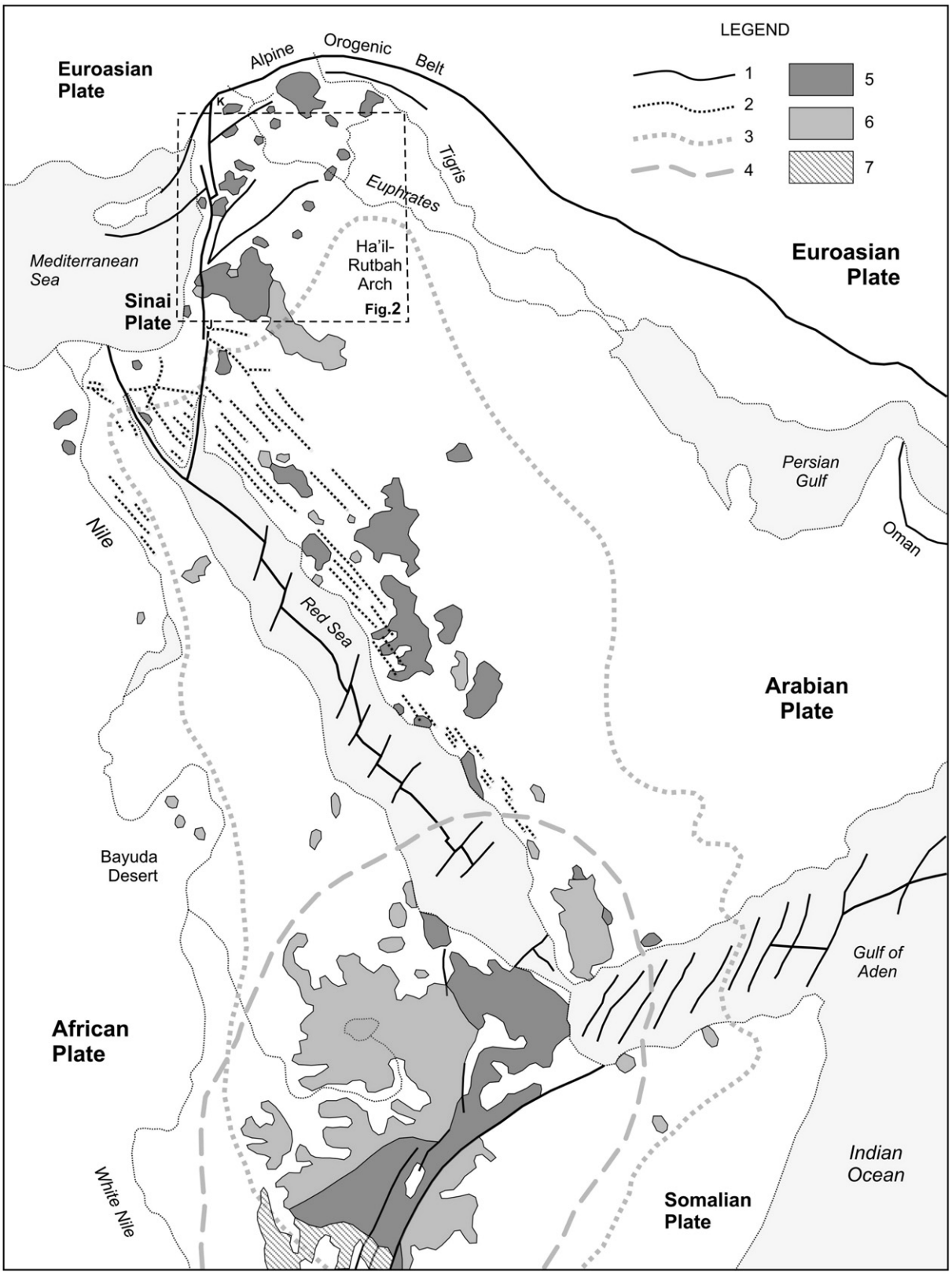

Fig. 1. The Ethiopia–Arabian plate volcanism (Segev, 2005). 1, main faults; 2, Middle Cenozoic dykes; 3, boundaries of the Afro-Arabian dome; 4, boundaries of the Ethiopia–Afar mantle plume; 5, Late Cenozoic volcanics; 6, Middle Cenozoic volcanics; 7, Early Cenozoic volcanics; J, site of collecting of the sample 22/3; and K, Kahraman-Maraş basaltic field.

However, Lustrino and Sharkov (2006) represented objections on links between the basalts and sub-lithosphere plumes: (1) "the spinel/garnet-bearing lherzolitic sources evidenced by semi-quantitative geochemical modeling can be related only to relatively shallow sources (generally <90 km in depth)" (p. 136), i.e., in the lower lithosphere; (2) no one-way age progression of magmatic activity and the long time span of eruptions in the same areas do not correspond to the deep mantle plume volcanism; and (3) the Sr and Pb isotopic ratio

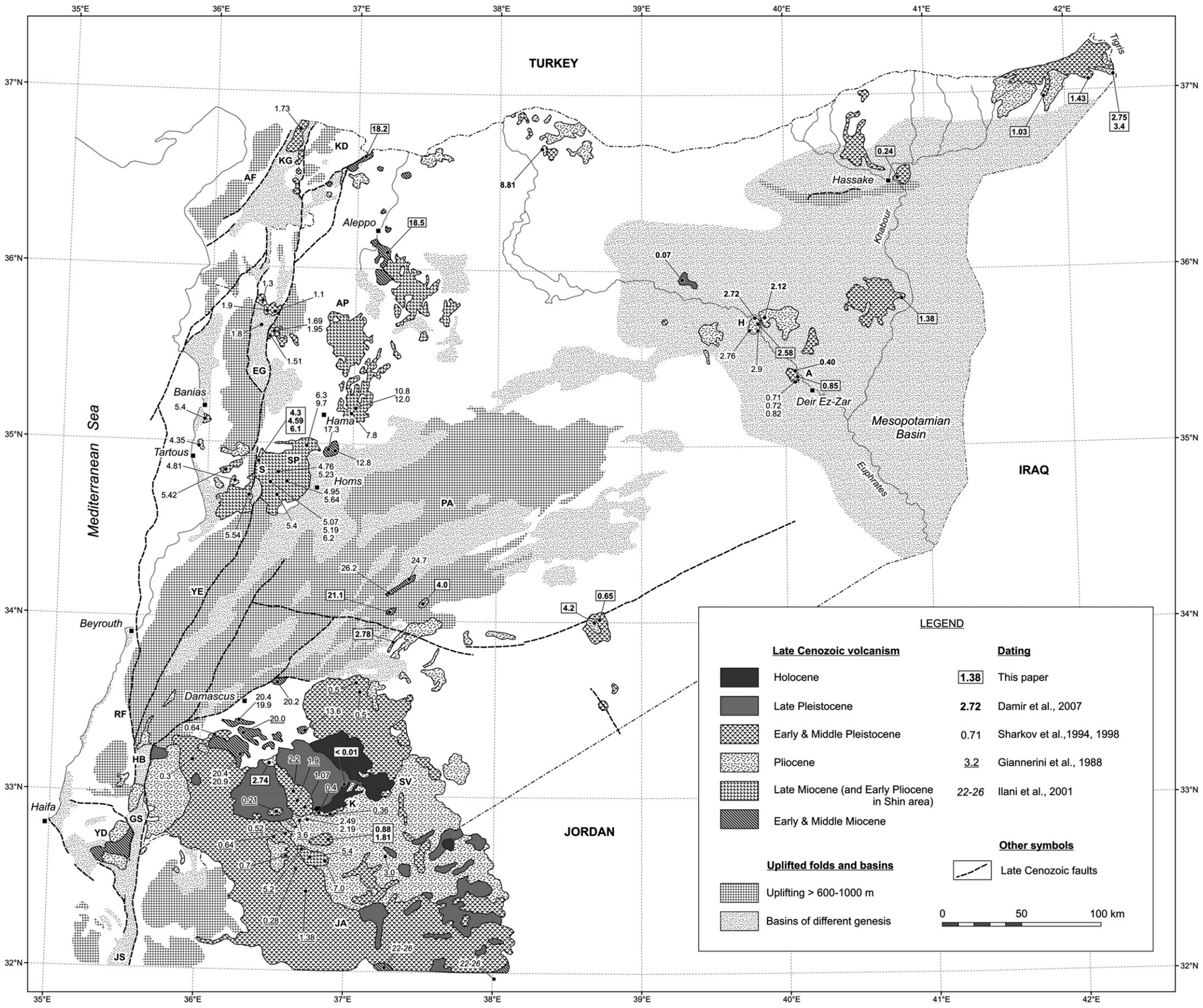

Fig. 2. Structural–geological map of Neogene–Quaternary basalts in Syria and adjacent territories. Structural features and basaltic fields: AF, Amanos fault (East Anatolian fault zone); AP, Aleppo Plateau; EG, El Ghab pull-apart basin, segment of the DST; GS, Galilee Sea pull-apart basin; HB, Hula pull-apart basin; JA, Jebel Arab (Harrat Ash Shaam) Highland; JS, Jordan Valley segment of the DST; KD, Kurd Dagh ridge; KG, Karasu graben; PA, Palmyrides; RF, Roum fault; SP, Shin Plateau; SV, Safa volcano; YD, Yizre'el depression; and YF, Yammuneh segment of the DST. Sites: A, Ayash village; H, Halabiyeh lava field; K, Kra lava field; and S, Saraya section.

differences exclude any participation of the Afar plume in generation of the central–northern Arabia basalts. Lustrino and Sharkov (2006) "propose that lithospheric extension is the main cause of igneous activity" and emphasize its "structural control by lithospheric discontinuities representing preferential pathways for uprising magmas" (p. 135). According to Weinstein's data, noted by Segev (2005), the Galilee–Dead Sea region basalts were lithosphere-derived and could have "two principal sources: amphibole-rich peridotite," related to the Late Proterozoic slab and "amphibole–garnet-rich pyroxenitic veins within the peridotite source, produced by the Paleozoic within-lithosphere partial melting event." Weinstein et al. (2006) linked the basalts with heat "from thermally anomalous zone within the sub-lithospheric mantle."

Contradiction of views to the basalt origin is caused by lack of the data on or attention to geological history of the volcanism and relationships between it and neotectonic evolution of the Arabian plate. A goal of this paper is to present new data on geology and K–Ar dating of the Late Cenozoic basalts in Syria, to outline a history of this volcanism by combined analysis of the new and previous data and to correlate it with neotectonic evolution and changes of geodynamic situation in the region. This gives a new view to origin of the basalts.

2. General geological and geochemical features of the Late Cenozoic basalts in Syria

The Late Cenozoic basalts are represented in Syria and the adjacent territories by multi-age lava flows, which often cover each other (Fig. 2). The basaltic tephra and spatter in and near volcanoes and pyroclasts and hyaloclasts are less distributed. The latter deposits have been observed in the DST grabens and near the Mediterranean coast. Dykes have been found in ruins of some volcanoes and in the lava flows on both sides of the DST.

The Jebel Arab Highland is situated in the southwestern Syria and continues to Jordan up to Saudi Arabia, where it is known as Harrat Ash Shaam. It is the largest Late Cenozoic basaltic field in the region. The maximum thickness of the basalts is >1200 m in the Syrian part of the Highland (Ammar, 1993; Rukieh et al., 2005). Its average height is ~700 m, but some volcanoes are 1000 m and even 1200–1800-m high in the central part of the Highland. Other basaltic fields are less in height and extent. One of them is the Shin Plateau in the eastern side of the DST to the west of the city of Homs. Analogous basalts are known there in the western side of the young strand of the DST and a part of them is continuous with the Shin basalts, offset sinistrally to 15–20 km on that strand (Chorowicz et al., 2004; Rukieh et al., 2005). Until the beginning of the Pliocene, the most active strand of the DST was represented by the Roum fault and its continuation on the continental slope (Trifonov et al., 1991; Barazangi et al., 1993; Rukieh et al., 2005). So, the basalts on both sides of the young DST strand were erupted on the Arabian plate. Relatively small basaltic flows are known in the Palmyrides and northern part of the Syrian Desert. The basalts are represented more in the Aleppo Plateau near the cities of Hama and Aleppo and continue from there to the north up to the Turkish town of Kahraman-Maraş (Çapan et al., 1987). Lava fields, formed by one or several flows are known in the Euphrates valley and in the northwestern part of the Mesopotamian Foredeep. Basalts of the northern margin of the Foredeep are continuous with the large basaltic fields in the southeastern Turkey.

In the DST zone, the Late Cenozoic basalts are exposed in the northern part of the El Ghab pull-apart basin and in the Karasu graben between the northern termination of the DST and the Amanos fault of the East Anatolian fault zone. Farther to the south, the basalts are exposed or are penetrated by bore holes in the Hula pull-apart basin and the Jordan valley and cover vast areas in the Yizre'el depression near the Galilee Sea (Garfunkel, 1989; Segev, 2005). The latter areas represent the western termination of the Jebel Arab lava field, offset sinistrally on the DST (Segev, 2005). Near the Dead Sea, the basalts are exposed in the eastern side of the DST and appear along its western side only near the Red Sea as a part of the Dyke Belt.

The Late Cenozoic basalts were erupted by small volcanoes, whose ruins are found in the basaltic fields. Some eruption centers are so morphologically inexpressive that their location was identified only by relative elevation of different parts of the lava surface and signs of flow, if the surface was preserved well. In the Jebel Arab Highland, fissure eruptions predominate. Centers of eruption form the NW-trending and NNW-trending linear chains, where some young volcanoes are joined by open fractures. So, the chains represent extensional faults. Some chains are formed by volcanoes of different ages, for example, the Late Miocene and Pliocene or Pliocene and Pleistocene. It demonstrates long duration and inheritance of the volcanic process, in contrast to basaltic volcanism in rift zones of Iceland as a part of the Mid-Atlantic ridge. The Icelandic linear volcanic chains acted for a short time (Trifonov, 1978). Linear location is characteristic also to volcanoes in the Shin Plateau (the NW–SE trend; Chorowicz et al., 2004). The N–S-trending groups of volcanoes are situated on the normal-sinistral faults or form short parallel chains in the northern part of the DST. Besides the fissure eruption zones, there are single small volcanoes and their nonlinear groups as well as rare shield volcanoes (as the Safa Holocene center) in the Jebel Arab Highland.

Composition of the Late Cenozoic Syrian basalts is generally similar to that of basalts in the adjacent parts of the Arabian plate (Alici et al., 2001; Shaw et al., 2003; Segev, 2005). The Syrian basalts are mostly high TiO_2 (1.8–3.7%) alkaline mafic rocks (basanites, hawaiites and alkali basalts) and rarer transition/tholeitic basalts with 44.3 to 52.5% of SiO_2. The Na_2O/K_2O ratios vary from ~1.5 to 5.6 and show positive correlation with the SiO_2 content (Sharkov et al., 1994; Sharkov, 2000; Lustrino and Sharkov, 2006). The $^{87}Sr/^{86}Sr$ ratios (0.70321 to 0.70485) show negative correlation with the $^{143}Nd/^{144}Nd$ ratios (0.512938 to 0.512842) (Lustrino and Sharkov, 2006). There are some peculiarities of basalt composition in different volcanic areas. The relatively high alkalinity is characteristic of basalts in the Shin Plateau and its coastal continuation, low alkalinity basalts predominate in the Jebel Arab Highland, while tholeites are typical of the southern Aleppo area (Sharkov, 2000).

Lustrino and Sharkov (2006) divided the Syrian basalts into two groups: (1) with ages between ~25 and ~5 Ma and (2) younger than ~5 Ma. In each group, content of the incompatible trace elements increases with decrease of the age as a result of fractional crystallization in magmatic sources. An abrupt change in basalt composition occurred ~5 Ma ago. That was decrease in TiO_2, Na_2O, K_2O, P_2O_5 and incompatible trace elements without decrease in MgO or increase in SiO_2. The authors above explain these phenomena by "increasing degree of partial melting and/or shallower depths of partial melting (i.e., increasing percentage of spinel in lherzolitic mantle)." By Lustrino and Sharkov (2006), the ~5 Ma adiabatic melting could follow the upper mantle decompression caused in turn by some re-organization in plate motions (Barazangi et al., 1993; Zanchi et al., 2002; Rukieh et al., 2005). It is worth noting however that the conclusion of Lustrino and Sharkov (2006) about the ~5 Ma event bases only on the data from the Shin Plateau and its coastal continuation, so that the event could have rather local than regional geodynamic cause.

The Late Cenozoic pyroclasts and some basalts contain mantle xenoliths of mainly the spinel lherzolites and the spinel and garnet–spinel vebsterites, and rare xenoliths of the pyroxene granulites, probably representing the old oceanic crust (Sharkov et al., 1996; Sharkov, 2000). That there are no xenoliths of the lower crust garnet granulites and of the upper crust material suggests that the intermediate magmatic sources were not characteristic of the Late Cenozoic volcanism.

3. Analytical methods

21 new K–Ar dates of the Syrian basalts and one date of the Jordanian basalt were obtained in 2006–2007 in the Laboratories of Isotope Geochemistry and Geochronology of the Institute of Geology

of Ore Deposits, Petrography, Mineralogy and Geochemistry of the Russian Academy of Sciences (*IGEM RAS*) and of the Geological Institute of the Russian Academy of Sciences (*GIN RAS*). The samples were collected during our field works in 2003, 2004 and 2007. Dating techniques were principally similar in both laboratories, but differed in some details.

In the Laboratory of IGEM RAS, the electromagnetic mineral separation was used for the samples 9.03/2, 326a/1, 326a/2, 326a/3, 424/2, 21.2004/1, and 28.2004/1 that had the porphyritic structure and contained a lot of plagioclase and olivine phenocrysts. As a result, the main part of the rock was separated from phenocrysts and used for the K–Ar dating. Content of potassium was measured with the photometer FPA-01 by the flame spectrophotometry technique. Accuracy was 1–3%. Content of the radiogenic argon was determined by technique of the isotope dilution with monoisotope ^{38}Ar as a spike. The measurements were carried out in the static regime using improved mass-spectrometric equipment, which was made in the *IGEM RAS* on the base of mass-spectrometer MI 1201 IG. Its Ar sensitivity is $5\cdot10^{-3}$ A/Torr, the total blank of analysis is $3\cdot10^{-3}$ ncm^3. Accuracy was controlled by systematic measurements of the $^{40}Ar_{rad}$ content in standard samples of "biotite-70A," muscovite "P-207" and muscovite "Bern-4M" as well as by measurements of air Ar isotope composition.

In the Laboratory of GIN RAS, content of potassium was measured with the atomic absorber AAS-3 with accuracy 1–1.5% and controlled by repeated measurements of "blind" samples and standards. Content of radiogenic argon was measured again by technique of the isotope dilution and monoisotope ^{38}Ar as a spike. Its composition corresponded to $^{40}Ar/^{38}Ar = 0.031$ and $^{36}Ar/^{38}Ar = 0.00131$. The measurements were carried out with the modified mass-spectrometer MI 1201 IG. Besides the standards, used in the *IGEM RAS*, the laboratory own standard "dacite-87" with the $^{40}Ar_{rad}$ content ~0.00288 mm^3/g was used for the accuracy control.

Both laboratories used the constants $\lambda_e = 0.581\times10^{-10}$ a^{-1}, $\lambda_\beta = 4.962\times10^{-10}$ a^{-1}, $^{40}K/K = 1.167\cdot10^{-4}$. The final errors were calculated as $\pm2\sigma$. All the data obtained are represented in Table 1. Table 2 describes geological position of each collected sample.

In parallel with K–Ar dating, G.Z. Gurariy (the Paleomagnetic Laboratory, *GIN RAS*) defined the residual magnetization of the basalts using a Czech magnitometer JR-4. All samples underwent standard thermal treatment by successive heating to 100° and 200° in the nonmagnetic space. Standard data processing showed that obtained paleomagnetic parameters do not usually contradict the K–Ar dates and sometimes correct them.

Some of the K–Ar dates were confirmed by geological data. For example, basalts with ages 18.2 ± 0.8 Ma (site 424) and 18.5 ± 0.8 Ma (site 21.2004) are overlain by limestone with Helvetian (Langhian + Serravallian) fossils, with the ~16.5 Ma lower age limit. Some K–Ar ages of Pleistocene basalts were controlled by archaeological dating of either underlying or covering sediments. The archaeological findings were particularly important for dating Holocene basalts.

4. New ages of Syrian Late Cenozoic basalts

First differentiation of basalts by their age was done in the course of geological mapping of Syria, in scale 1:200,000 (Geological Map of Syria, 1964). The further studies, K–Ar (Giannérini et al., 1988; Mouty et al., 1992; Sharkov et al., 1994, 1998) and ^{40}Ar–^{39}Ar (Demir et al., 2007) dating corrected chronology of the basalts. At the same time, many basaltic fields have remained undated, and this impelled us to continue the studies. We corrected distribution of Holocene basalts in the Jebel Arab Highland, carried out the K–Ar dating and paleomagnetic studies of some lava flows, studied relationships of the flows with bedrock and capping layers.

4.1. The Holocene volcanism

As the 1:200,000 geological maps show, large parts of the Jebel Arab Highland are covered by Holocene lavas (Geological Map..., 1964; Ponikarov et al., 1967). Our studies show that lava flows vary in how much their initial surface have been modified or preserved. We found the Late Paleolithic flint tool on the lava surface at N33°10.53′, E36°29.61′, *H* = 637 m. Obviously, the lava flow as well as other flows

Table 1
New K–Ar dates of the Neogene and Quaternary basalts, Syria (21 samples) and Jordan (1 sample).

No. lab	No. field	Latitude N	Longitude E	Alt. (m)	Material	K (%) ± σ	$^{40}Ar_{rad}$, mm^3/g, 10^5, ±2σ	$^{40}Ar_{air}$ (%)	Age (Ma ± σ)	p/m
G-1076	2.03	33° 10.53′	36° 29.61′	873	Basalt	0.39	4.16 ± 0.1	70	2.74 ± 0.10	R
G-1081	3.03/1	32° 41′ 35″	38° 54′ 06″	1141	Basalt	1.14	3.87 ± 0.08	40	0.878 ± 0.029	R
G-1080	3.03/2	32° 41′ 35″	38° 54′ 06″	1141	Basalt	0.56	3.93 ± 0.08	56	1.81 ± 0.05	N
G-1075	4.03	33° 52.15′	37° 16.82′	873	Basalt	0.74	8.00 ± 0.16	44	2.78 ± 0.08	
G-1079	6.03	35° 24.33′	40° 04.19′	210	Basalt	0.91	3.01 ± 0.09	75	0.85 ± 0.03	N?
G-1073	7.03	35° 42.06′	39° 49.04′	325	Basalt	0.91	9.35 ± 0.19	55	2.58 ± 0.08	N?
G-1082	8.03	34° 05.97′	37° 29.57′	968	Basalt	1.01	15.75 ± 0.32	46	4.00 ± 0.14	
G-1077	25.2004	37° 03.65′	42° 10.21′	745	Basalt	0.59	3.28 ± 0.08	75	1.43 ± 0.05	R?
G-1072	27.2004	36° 58.64′	41° 50.21′	–	Basalt	0.68	2.72 ± 0.07	61	1.03 ± 0.05	
G-1078	29.2004	35° 50.46′	40° 49.95′	280	Basalt	0.71	3.81 ± 0.08	32	1.38 ± 0.05	
G-1074	30.2004/3	34° 00.16′	38° 41.51′	775	Basalt/d	0.94	2.38 ± 0.07	77	0.65 ± 0.1	
G-1083	22/3	31° 44′ 10.3″	35° 35′ 58.3″	−336	Basalt/J	1.33	5.27 ± 0.11	38	1.02 ± 0.04	
No. lab	No. field	Latitude N	Longitude E	Alt. (m)	Material	K (%) ± σ	$^{40}Ar_{rad}$, ng/g ± σ,	$^{40}Ar_{air}$ (%)	Age (Ma ± σ)	p/m
I-13846	9.03/2	34° 02′ 11.2″	37° 16′ 13.2″	949	Basalt	1.04 ± 0.02	1.529 ± 0.011	70.6	21.1 ± 0.9	
I-13847	326a/1	34° 52′ 58.8″	36° 20′ 09.8″	827	Basalt	1.09 ± 0.02	0.461 ± 0.007	61.8	6.1 ± 0.3	N?
I-13848	326a/2	34° 52′ 58.8″	36° 20′ 09.8″	870	Basalt	0.96 ± 0.015	0.305 ± 0.003	44.8	4.59 ± 0.17	N
I-13849	326a/3	34° 53′ 24.1″	36° 19′ 54.4″	950	Basalt	0.80 ± 0.015	0.241 ± 0.004	50.1	4.3 ± 0.2	
I-13850	424/2	36° 34′ 27.9″	36° 58′ 00.4″	590	Basalt	1.05 ± 0.02	1.329 ± 0.017	55.2	18.2 ± 0.8	
I-13851	21.2004/1	36° 04′ 38.7″	37° 13′ 55.9″	470	Basalt	0.50 ± 0.015	0.648 ± 0.004	35.6	18.5 ± 1.0	
I-13852	26.2004/1	37° 05′ 22.1″	42° 20′ 43.5″	411	Basalt	0.40 ± 0.015	0.093 ± 0.0012	81.2	3.4 ± 0.3	N?
I-13853	26.2004/2	37° 05′ 22.1″	42° 20′ 43.5″	418	Basalt	0.50 ± 0.015	0.096 ± 0.0015	68.4	2.75 ± 0.19	R?
I-13854	28.2004/1	36° 30′ 57″	40° 46′ 56″	–	Basalt	0.95 ± 0.015	0.0156 ± 0.0018	92.1	0.24 ± 0.06	
I-13855	30.2004/1	34° 00′ 05.1″	38° 41′ 24.4″	722	Basalt	0.65 ± 0.015	0.191 ± 0.005	91.0	4.2 ± 0.3	

G — dated in the Laboratory of Isotope Geochemistry and Geochronology of the Geological Institute of the Russian Academy of Sciences (GIN RAS); I — dated in the Laboratory of Isotope Geochemistry and Geochronology of Institute of Geology of Ore Deposits, Petrography, Mineralogy and Geochemistry of the Russian Academy of Sciences (IGEM RAS); d — dyke or neck; all other samples were collected in lava flows; J — sample, collected in Jordan; all other samples were collected in Syria. Paleomagnetic polarity (p/m): N — normal, R — reverse.

Table 2
Geological position of the samples collected for the K–Ar dating, Syria and Jordan.

No. field	Date	Coordinates	Short description	Comments
2.03	29.10.03	N33°10.53′ E36°29.61′ $H=873$ m	Basalt, covered by the terrigeneous deposits.	K–Ar = 2.74 ± 0.10, p/m = R
3.03	29.10.03	N32°41′35″ E38°54′06″ $H=1141$ m	2 basaltic flows: (1) upper and (2) lower.	Upper: K–Ar = 0.878 ± 0.029, p/m = R. Lower: K–Ar = 1.81 ± 0.05, p/m = N
4.03	2.11.03	N33°52.15′ E37°16.82′ $H=873$ m	Basalt	K–Ar = 2.78 ± 0.08
6.03	4.11.03	N35°24.33′ E40°04.19′ $H=210$ m	Quarry to the SE of village of Ayash. The 3-m basaltic flow covers alluvium of the 20–25 m Euphrates terrace with the Acheulian tools.	K–Ar = 0.85 ± 0.03, p/m = N?. The former our K–Ar dates: 0.71 ± 0.08, 0.72 ± 0.08, 0.82 ± 0.07 (Sharkov, 2000)
7.03	4.11.03	N35°42.06′ E39°49.04′ $H=325$ m	Village of Halabiyeh. The ~100 m Euphrates terrace. 2 basaltic flows (15 m totally) cover thin alluvium pebbles, which cover the Tortonian. The sample is collected in 1/3 from the basalt bottom.	K–Ar = 2.58 ± 0.08. p/m = N? from the top of the basalts. The former K–Ar and Ar–Ar dates ≈ 2.7–2.8 (Sharkov, 2000; Demir et al., 2007)
8.03	6.11.03	N34°05.97′ E37°29.57′ $H=968$ m	Basalt in the top of a hill. The Levallois technique material in the top of the basalt.	K–Ar = 4.00 ± 0.14
9.03	6.11.03	N34°02.25′ E37°15.91′ $H=949$ m	Basalt up to 100 m covers the Maastrichtian.	K–Ar = 21.1 ± 0.9 near the top
326a	11.11.03	Bottom: N34°52′58.8″ E36°20′09.8″ $H=827$ m. Top: N34°53′24.1″ E36°19′54.4″ $H=950$ m	Saraya to the NW of village of Bolshin. The ~120 m basaltic section covers the Cenomanian.	K–Ar in the lower part = 6.1 ± 0.3, p/m = N? K–Ar in the middle = 4.59 ± 0.17, p/m = N. K–Ar in the top = 4.3 ± 0.2
424	21.03.04	N36°34.50′ E36°57.94′ $H=590$ m	Basalt (≥5 m) is covered by clay (2.5 m) that is covered by conglomerate (3.5 m, up to 4–5 m) with ophyolite debris and the limestone lense in the lower part.	K–Ar = 18.2 ± 0.8
21.2004	21.03.04	N36°04.68′ E37°13.87′ $H=470$ m	Basalt (≥5 m) is covered by the Helvetian limestone.	K–Ar = 18.5 ± 1.0
25.2004	23.03.04	N37°03.65′ E42°10.21′ $H=745$ m	Basalt covers the Bakhtiari Formation with unconformity 3°.	K–Ar = 1.43 ± 0.05, p/m = R?
26.2004	23.03.04	N37°05.42′ E42°20.66′ $H=411$ m	The 20-m Tigris terrace ($H=320$–325 m). The 70–80-m Tigris terrace ($H=363$ m). Higher in the slope upward: (1) Bakhtiari conglomerate, >20 m; (2) weathered basalt, 3 m; (3) the Bakhtiari conglomerate, 1 м; (4) unknown, 5 m; and (5) basalt, ≥10 m (the top = ~430 m).	Basalt (2) K–Ar = 3.4 ± 0.3, p/m = N? Basalt (5) K–Ar = 2.75 ± 0.19, p/m = R?
27.2004	23.03.04	N36°58.64′ E41°50.21′	Basalt	K–Ar = 1.03 ± 0.05
28.2004	24.03.04	N36°30.52′ E40°46.56′	Left (eastern) bay of the El-Khabour River. Upward: (1) loam, 2 m; (2) basalt, 4 m; and (3) the Late Quaternary loam.	Basalt (2) K–Ar = 0.24 ± 0.3
29.2004	24.03.04	N35°50.46′ E40°49.95′ $H=280$ m	Basalt (≥10 m) covers clays and aleurolites of the N_1^3	K–Ar = 1.38 ± 0.05
30.2004	25.03.04	N34°00.16′ E38°41.51′ $H=775$ m	Basalts form the N-trending small volcanic ridge.	K–Ar of the basalt 1 in bottom = 4.2 ± 0.3. K–Ar of the basaltic dyke 3 within the ridge = 0.65 ± 0.10
22/3	04.04.07	N31°44′10.3″ E35°35′58.3″ $H=-336$ m	The NE coast of Dead Sea. Basalt covers the statificated unit of pebbles and loam of the Dead Sea terrace.	K–Ar = 1.02 ± 0.04

with the same degree of initial surface preservation must be Pleistocene in age. Less intact flows can be then of the Holocene age. For example, basalts of the Kra lava field cover the Middle–Upper Pleistocene caliche and alluvium of the Kra Wadi and, thus, erupted in the Holocene (Trifonov, 2007). New data, obtained by Karakhanian, Trifonov, Dodonov and Bachmanov in 2007–2008, showed that this field consists of lava flows of different age. Besides the Early Holocene generations with the Neolithic artifacts on the surface, there are younger flows, which erupted from small volcanoes within the lava field and covered constructions and signs of inhabitation dated archaeologically as of Neolithic, Chalcolithic and even Early Bronze Age. The most recent flows can be dated back to the beginning of the second half of the III millennium BC (Trifonov and Karakhanian, 2008). Simkin and Siebert (1994) mention that the Safa volcano erupted in XVII century AD.

4.2. The Pleistocene volcanism

New data were obtained in the Euphrates River valley. According to our previous data, SE of the village of Ayash (10 km to the NW of the town of Deir Ez-Zor), the 20–25-m high Euphrates terrace exposed in a quarry, is covered by the 3-m thick basaltic flow (Devyatkin and Dodonov, 2000). Three K–Ar dates of the basalt range from 0.71 ± 0.08 Ma to 0.82 ± 0.07 Ma, that is, give roughly 0.8–0.7 Ma (Sharkov et al., 1998; Sharkov, 2000). The new K–Ar date of 0.85 ± 0.03 Ma (6.03 in Tables 1 and 2) seems to be an overestimation, since the basalt shows normal magnetic polarity. Artifacts found in the alluvium were assigned to the Late Acheulian with elements of the "Levallois-like" technique (Besançon and Sanlaville, 1981; Muhesen, 1985). Demir et al. (2007) studied the ~8-m river terrace in one terrace sequence with the 20–25-m

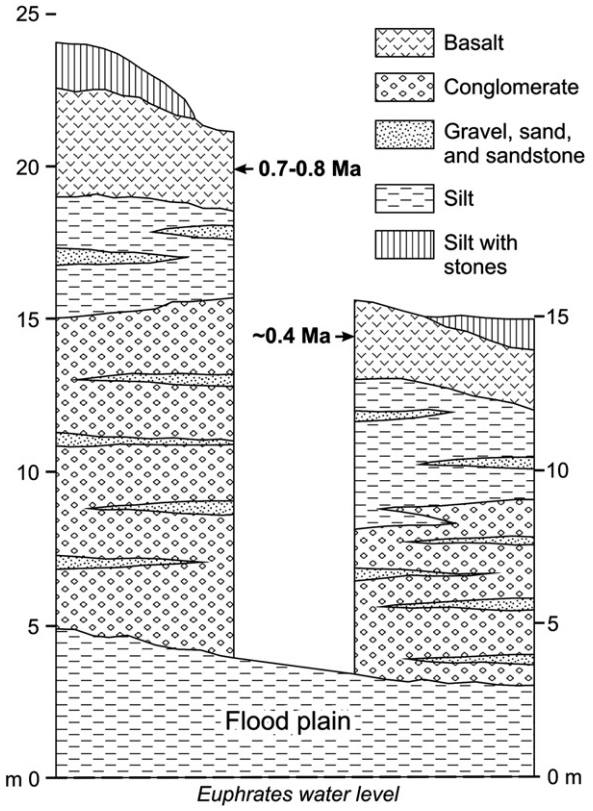

Fig. 3. Sections of the 20–25-m and the 8–15-m Euphrates terraces and the covering basalts near the village of Ayash.

terrace. They found that both terraces are mantled with a single basaltic flow, but differ in artifacts. The lower terrace contains the "Levallois-like" material, interpreted as Middle Paleolithic, while the upper terrace yields the Upper Acheulian material. ^{40}Ar–^{39}Ar dating of basalt on the lower terrace gave 410.6 ± 14.6 Ka and 389.9 ± 17.0 Ka, that is, about 0.4 Ma (Demir et al., 2007).

So, our previous and Demir et al. (2007) dates of the basalts, and the age estimates of artifacts from the upper terrace contradict to each other. We visited the area again in 2008 and found that basalts on the upper terrace and the lower terrace belong to flows from different volcanoes. The upper (~23 m) terrace (the quarry SE of Ayash) is composed of (top-down, Fig. 3):

(1) basaltic flow, dated ~0.8–0.7 Ma, ~3-m thick (in places covered by up to 2 m of recent silt) (Fig. 4C);
(2) silt with lenses of coarse material — 2–4 m in thickness; and
(3) fluvial loose conglomerates (several layers, pebbles and boulders rounded, lenses of fine material, horizontal or oblique stratification) containing sand dykes (Fig. 4A and B) and artifacts of the Acheulian type — up to 10-m thick (visible).

The lower terrace (~15-m high) contains in the northern margin of Ayash (top-down, Figs. 3 and 4D):

(1) basaltic flow, dated by Demir et al. (2007) to be ~0.4 Ma old, covered by 1 to 2 m of recent silt within a depression up to 2 m deep on the flow surface — ~3-m thick;
(2) silt with lenses of coarse material — up to 5 m in thickness; and
(3) dark-gray horizontally stratificated fluvial gravel with thin lenses of fine material — up to 6-m thick (visible).

The floodplain (3–5 m above the Euphrates level) incised into both terraces is composed of dark-gray clay and silt.

The obtained data and their comparison with the results of Demir et al. (2007) show that the I and II terraces near village of Ayash are covered by basalts of different ages, ~0.4 Ma and ~0.7–0.8 Ma, respectively. Artifacts of the "Levallois-like" type were found in the lower terrace sediments. Artifacts within the upper terrace alluvium are, obviously, older than the Late Acheulian.

4.3. The Late Miocene to Early Pleistocene volcanism

Three K–Ar dates of the Saraya section in the eastern side of the DST are important for understanding the Shin Plateau structure. Geological and paleomagnetic studies of the section were carried out earlier (Trifonov et al., 1991). The section is ~120-m thick and contains 12 lava flows (Fig. 5). The K–Ar age of the upper flow is 4.3 ± 0.2 Ma, and the age of the flow, located ~1/4 above the section base is 6.1 ± 0.3 Ma. Probably, the section corresponds mainly to the paleomagnetic anomalies *3r–3br*, although the lowest flow can be older.

The Saraya basalts cover the eroded surface of the Cenomanian limestones in the eastern limb of the Coastal anticline. The basaltic field is offset 15–20 km left-laterally on the young strand of the DST, if counted relative to similar basalts in the western side of the strand, which corresponds to the axial part of the anticline. The basalts west of the DST strand cover the Jurassic limestones. This means that the anticline formed and then was eroded before the basaltic eruptions, and that erosion removed ~500 m of sediments from the axial part of the anticline, compared with its eastern limb. That lavas cover wide areas, and their fields are generally isometric in plan-view, suggest that basalts erupted onto a relatively flat ground surface, which truncates the anticline. Due to later anticline growth, portion of the lava field elevated to different present altitudes. Near Kal'at Markab, south of Banyas, the 5.4 ± 0.2 Ma old basalts erupted onto the erosion surface on the Cenomanian–Turonian limestones of the western limb of the Coastal anticline. Father west, basalts cover the Late Miocene–Early Pliocene marine sediments (Kopp and Leonov, 2000). There they erupted likely off shore, near the sea coast, as their hyaloclastic appearance suggests. Since the eruption, the basalts and hyaloclasts have elevated to present altitudes of 260–300 m. SE of this site, in the axial part of the anticline, 5.4–4.8 Ma old basalts rest now at altitudes of up to 800 m. East of the DST (the western part of the Shin Plateau), roofs of the basalts are not usually higher than 400 m of present altitude and their bedrock is situated 100 to 200 m lower. This area corresponds to the eastern limb of the anticline, where the main centers of eruption were situated.

The Halabiyeh lava field is situated in the right side the Euphrates valley, between the towns of Ar Raqqa and Deir Ez-Zor. Near the village of Halabiyeh and the Roman fortress, the ~15-m thick basalt, composed probably of several lava flows, covers the ~80–100-m high river terrace. Earlier, we obtained two K–Ar dates of the basalts: 2.9 ± 0.1 Ma and 2.76 ± 0.09 Ma (Sharkov et al., 1998; Sharkov, 2000). The new K–Ar date of the upper flow (7.03 in Tables 1 and 2) is 2.58 ± 0.08 Ma. Demir et al. (2007) reported two ^{40}Ar–^{39}Ar dates obtained for the divided sample of the same basalt: 2764.8 ± 29.3 and 2676.4 ± 27.2 Ka. So, all the dates give the age of ~2.8–2.65 Ma. The basalts cover fluvial conglomerate, several meters thick, and the underlying Tortonian deposits.

In the northern part of the Halabiyeh basaltic field near the village of Al Kasaba, a height of the terrace (with the basalts) is ~110–120 m. The basalts (~24 m) cover the ~12-m thick fluvial gravel and underlying Tortonian deposits. In spite of the Demir et al. (2007) data, the nearby 60-m high terrace is not covered by the basalts.

Fig. 4. Details of the 20–25-m and the 8–15-m Euphrates terraces: A, the sand dykes, which cut the lower conglomerate layer and are covered by the upper conglomerate layer within the unit 3 of the 20–25-m Euphrates terrace in the quarry to the SE of the village of Ayash; B, the sand dyke, which cuts and deform the unit 3 of the same terrace in the quarry; C, the basalt 1, covering the unit 2 of the same terrace in the quarry; and D, the units 1–3 of the lower terrace section in the village of Ayash.

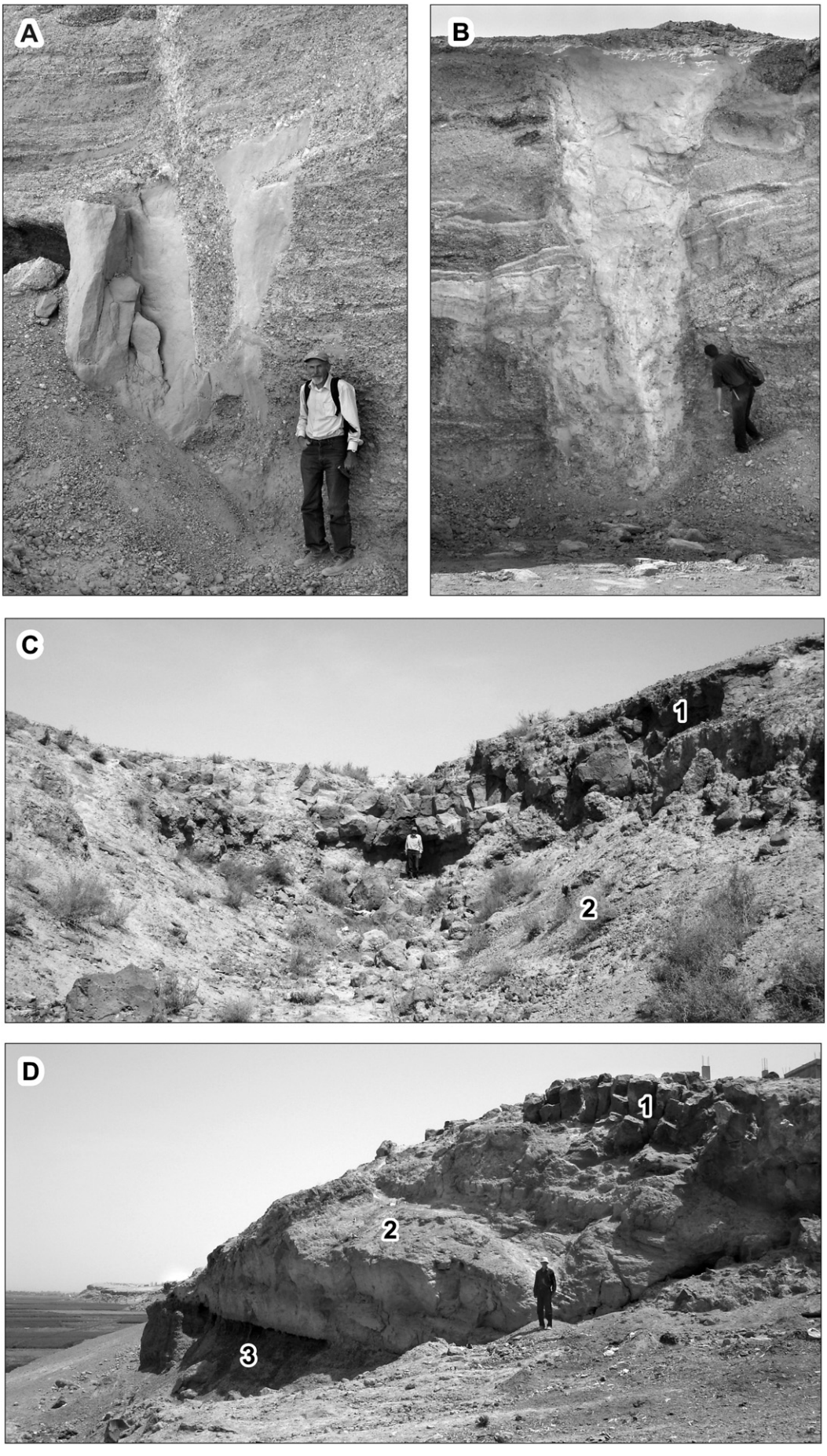
A
B
C
1
2
D
1
2
3

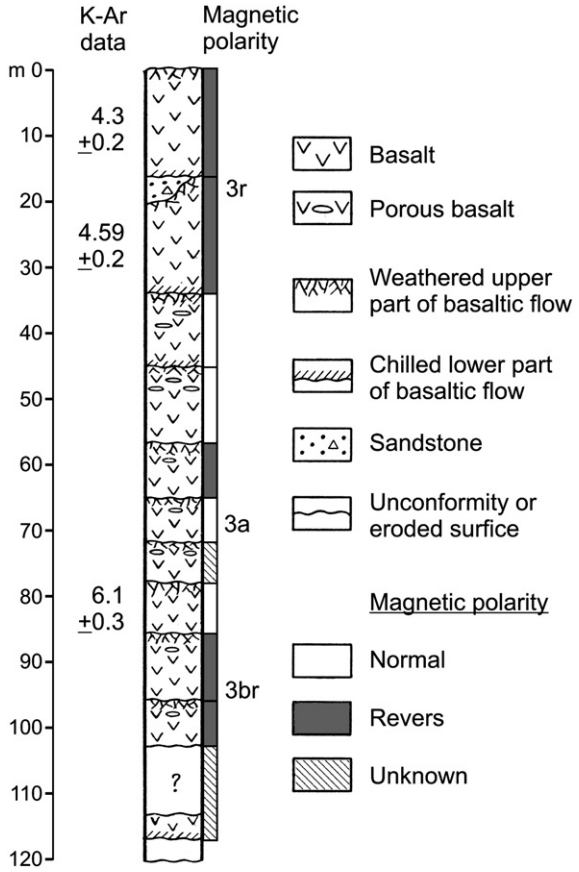

Fig. 5. A section of the Upper Miocene and Lower Pliocene basalts in Saraya, eastern side of the Dead Sea Transform, the western Syria.

In the NE of Syria near the Tigris River, two river terraces have been identified: ~20 m (altitude is 320–325 m) and 70–80 m (altitude is ~363 m). The following section is exposed above the terraces: (1) Bakhtiari conglomerate, >20 m in thickness; (2) weathered basalt, 3-m thick, with the K–Ar age of 3.4 ± 0.3 Ma (26.2004/1 in Tables 1 and 2, normal (?) magnetic polarity); (3) Bakhtiari conglomerate, 1 м thick; (4) not exposed, 5 m; and (5) basalt, ≥10 m, with the K–Ar age of 2.75 ± 0.19 Ma (26.2004/2 in Tables 1 and 2; reverse (?) magnetic polarity). The top of the section lies at altitude of ~430 m. The basalt, covering the Bakhtiari Formation with 3° unconformity, is dated to be 1.43 ± 0.05 Ma old.

5. Late Cenozoic history of Syrian volcanism and tectonic evolution of the region

The new ages of the basalts together with 71 earlier K–Ar and ^{40}Ar–^{39}Ar age determinations (Giannérini et al., 1988; Sharkov et al., 1994, 1998; Sharkov, 2000; Demir et al., 2007) give a possibility to correct the map of basalts (Fig. 2), to outline a history of the Late Cenozoic Syrian volcanism and correlate it with tectonic structure and evolution.

Structural links between volcanism in the northwestern Arabia and the DST are manifested by location of volcanoes along the N-trending border and inner faults in the Karasu, El Ghab and Hula pull-apart basins as well as along the Jebel Arab and Shin NNW-trending extensional faults, which can be interpreted as associated with the sinistral DST. Some other Late Cenozoic volcanoes and lava fields do not demonstrate any links with the DST or other crustal structures of the Arabian plate. At the same time, there is some correlation between periodicity in volcanism activity and structural evolution of the plate boundaries (Table 3).

Four stages of neotectonic evolution were identified in active zones surrounding the Arabian plate (Kaz'min, 1974; Savostin et al., 1986; Rukieh et al., 2005). Each of them had its own characteristics basically defined by plate relative movements in the region, and, first of all, by direction of opening in the Aden–Red Sea rift system. The rift system was originated in Oligocene when the belt of parallel dykes, small volcanoes and extrusions formed 32–20 Ma in the northeastern side of the Red Sea rift (Camp and Roobol, 1992; Segev, 2005). During the first, Late Oligocene–Early Miocene, stage, the rift system propagated to the west and, subsequently, its eastern part could undergo larger extension than the western part. As a result, the Arabian plate moved to the NNW and produced sinistral slip on the DST and shortening in the northwestern margin of the plate. The DST was originated in the Early Miocene (20–17 Ma). Its southern part offsets sinistrally the Dyke Belt (Garfunkel and Ben-Abraham, 2001; Hurwitz et al., 2002). During the first stage, the northern part of the DST followed along the Roum fault and farther north along the continental slope reaching the convergent portion of the plate boundary in the north (the Latakia thrust with the sinistral component and the Taurus thrusts (Trifonov et al., 1991; Barazangi et al., 1993; Rukieh et al., 2005)).

In the second, Middle Miocene, stage, the Red Sea rift was opening faster than the Aden rift, causing the Arabian plate to move to the NE. This resulted in intensive motion on the Main Thrust of Zagros, initiation and development of the Mesopotamian Foredeep, and the beginning of folding in its northeastern margin. No essential deformation took place in the northwestern Arabia.

Acceleration of tectonic movements took place in the Aden–Red Sea rift system on the third stage, in the Late Miocene and particularly Messinian. It probably reflected the break-up of the continental crust and the onset of spreading (Kaz'min, 1974; Izzeldin, 1987). The break-up occurred in the Aden rift earlier, than in the Red Sea rift, and the Arabian plate moved to the NNW because of it. This resulted in folding and thrusting in the Palmyride belt.

In the fourth, Middle Pliocene–Quaternary, stage, spreading propagated into the Red Sea rift. It caused the northern drift of the Arabian plate and N–S shortening along its convergent boundaries. Re-organization of the northern part of the DST occurred between the third and fourth stages when its new Yummuneh and El Ghab strands formed. The El Ghab strand joined in the north with the newly formed East Anatolian fault zone (Zanchi et al., 2002; Rukieh et al., 2005).

The Late Cenozoic volcanic area forms the N-trending band, which extended in the western part of the Arabian plate approximately parallel to the DST. Most of magmatic channels, marked by volcanic chains, strike here NNW–SSE and can be interpreted as extensional faults associated with the left-lateral DST zone. The NNW–SSE compression, characteristic for the first and third stages, was accompanied by the ENE–WSW extension. This favoured opening of extensional faults and volcanic activity. The oldest basalts with the K–Ar ages of 26–20 Ma were found in Harrat Ash Shaam (Ilani et al., 2001) and its northern surroundings (Fig. 2). In 19 to 17 Ma, the eruptions occupied the belt farther north, up to the southeastern Turkey (Arger et al., 2000; Tatar et al., 2004). Eruptions resumed in the same belt during the third stage. During the second stage, with NE–SW-directed compression and NW–SE-directed extension, volcanism waned in Syria and ceased in the Jordanian part of Harrat Ash Shaam. Decrease in volcanic activity started in the north later (~17 Ma) than in the south (~20 Ma), as seen in distribution of dated basaltic flows (Fig. 6).

The important feature of the end of the third stage was spreading of volcanism ~6.3–4 Ma into the Shin Plateau and its western continuations near the towns of Tartous and Banyas. Geochemical features of the Shin basalts described above differ them from other basalts and suggest either the higher degree or a shallower depth of partial melting, i.e., decompression in the mantle source (Lustrino and Sharkov, 2006). It may be thought that formation of the source of the Shin lavas somehow related to shortening in the Palmyrides. A probable scenario implies that, together with sinistral motion on the

Table 3
Volcanism in the northwestern part of the Arabian plate in comparison with stages of tectonic evolution in the plate boundary zones.

Stage	Age of the stage	Aden–Red Sea rift system	Direction of the plate drift	DST	Convergent plate boundaries	Volcanism
1	Oligocene–Early Miocene	Two phases of rifting: 35–30 Ma and 25–20 Ma (11). Propagation of rifting to the west. As a result, the Aden rift extended more intensively, than the Red Sea one.	NNW	Formation of the southern segments 20–17 Ma (4, 5). They continued to the north by the Roum faults and northward along the continental slope (2, 9, and 15). Sinistral slip on the DST.	Marine regression in North Arabia (8). Acceleration of folding and thrusting in the northwestern plate boundary at ~17 Ma (9).	Formation of dykes, small volcanoes and extrusions along the northeastern side of the Red Sea rift: from 32–30 Ma until ~20 Ma with maximum 24–21 Ma in Saudi Arabia (3) and from 24.8 ± 1.5 until 20.3 ± 0.7 Ma in Sinai (11). Origination of relatively narrow N-trending volcanic band in Western Arabia in Oligocene; the K–Ar dates 26–22 Ma in Harrat Ash Shaam (6) and 26.2 ± 2.1 and 24.7 ± 1.4 Ma in the western part of the Ed Dau basin in Palmyrides (12). Continuation of the band activity and its propagation to the northwestern Syria (Fig. 2) and the southeastern Turkey, Kahraman-Maraş lava field with the K–Ar dates from 19.1 ± 1.3 Ma until 16.5 ± 0.6 Ma (1, 14).
2	Middle Miocene	The Red Sea rift extended more intensively, than the Aden one	NE	Tectonic "quiescence" in the northwestern Arabia	Thrusting on the Main Thrust of Zagros; formation of Mecopotamian Foredeep in front of it; beginning of folding in the northwestern side of the Foredeep.	Very rare eruptions with K–Ar ages between 17 and 12 Ma in Syria (Fig. 2) and Saudi Arabia (3). Hiatus of volcanism in Harrat Ash Shaam (6). Formation of the 630–650-m Lower Basalt Group with the ^{40}Ar–^{39}Ar and K–Ar dates ~16–10 Ma in the Yizre'el depression between the Galilee Sea and the Haifa fault (Fig. 2) (11).
3	Late Miocene–Early Pliocene	Beginning of spreading in the Aden rift	NNW	Renewal of sinistral slip on the former stands.	Folding and thrusting in Palmyrides, accelerated in the Messinian	Renewal of eruptions in the Syrian part of the N-trending band in 12–7 Ma. Activation of volcanism in ~6.3–4 Ma in the N-trending band, including the Shin Plateau and its western extension. In the Jordanian part of Harrat Ash Shaam, volcanism was resumed ~13 Ma and continued until 3 Ma with brief hiatus ~7 Ma (6). In the Yizre'el depression, wane of volcanism for ~9–6 Ma gave place to eruptions of the 55–175-m Cover Basalt (Bashan Group) with the ^{40}Ar–^{39}Ar dates from 5.1 ± 1 until 3.5 ± 0.1 Ma (11).
4	Middle Pliocene–Quaternary	Propagation of spreading into the Red Sea rift	North	Re-organization of the northern part of the DST (4–3.5 Ma): formation of the Yammuneh strand and the El Ghab strand, which joined with the East Anatolian fault zone (9, 17).	Shortening on the northern plate boundary; sinistral (with reverse component) motion on the East Anatolian fault zone and dextral (with reverse component) motion on the Main Recent fault of Zagros.	Brief hiatus of volcanism in 4–3.5 Ma. The further activation of volcanism in the N-trending band, which spread to the east up to the northwestern part of the Mesopotamian Foredeep and to the west into the recent DST zone (Fig. 2). In the DST zone, volcanoes were located on the N-trending boundary and inner faults of the Karasu valley (~2–0.4 Ma), the El Ghab pull-apart basin (from 1.9 ± 0.1 until 1.1 ± 0.2 Ma), the Hula pull-apart basin and the Jordan valley (from 2.16 ± 0.28 until 0.95 ± 0.03 Ma) (11, 12, 13, and 16).

References: (1) Arger et al., 2000; (2) Barazangi et al., 1993; (3) Camp and Roobol, 1992; (4) Garfunkel and Ben-Abraham, 2001; (5) Hurwitz et al., 2002; (6) Ilani et al., 2001; (7) Kaz'min, 1974; (8) Krasheninnikov, 2005; (9) Rukieh et al., 2005; (10) Savostin et al., 1986; (11) Segev, 2005; (12) Sharkov, 2000; (13) Sharkov et al., 1994; (14) Tatar et al., 2004; (15) Trifonov et al., 1991; (16) Yürür and Chorowicz, 1998; and (17) Zanchi et al., 2002.

DST, the shortening caused the NE-directed movement of the Aleppo block and subsequent decompression in the southwestern part of the block, resulted in the Shin volcanism. These changes in the lithosphere caused rebuilding of the northern part of the DST. New strand of the DST formed in the Shin area. It became the main strand and propagated to the south (Yammuneh segment) and to the north (El Ghab segment) up to junction with the newly formed East Anatolian fault zone (Zanchi et al., 2002; Rukieh et al., 2005). The moment of rebuilding of the DST system was manifested by brief wane of volcanism ~4–3.5 Ma.

A sequence of the Miocene–Early Pliocene volcanic events near the Galilee Sea and in the Yizre'el depression repeated the Syrian "scenario" with some delay. Voluminous eruptions occurred there ~16–10 Ma and in the interval between 5.1 ± 0.1 and 3.5 ± 0.1 Ma, with an epoch of low volcanic activity in-between (Segev, 2005). Perhaps, this depended on location of the depression in the area of the two major faults junction where the geodynamic changes were manifested by other way, than in the Arabian plate.

The N–S-trending compression and the W–E-trending extension favoured volcanic activity during the fourth stage. Volcanism resumed, became more intensive in the Middle Pliocene and continued to the Late Pliocene, Pleistocene, and locally Holocene. This volcanism occupied the Jebel Arab Highland and spread to the east, into the northern part of the Syrian Desert, the Euphrates valley and the northern margin of the Mesopotamian Foredeep near the Turkish–Syrian boundary. No evidence for one-way rejuvenation of eruptions has been found. For example, the Middle and Late Pliocene and Early and even Middle Pleistocene (0.24 ± 0.06 Ma) erupted nearly at the

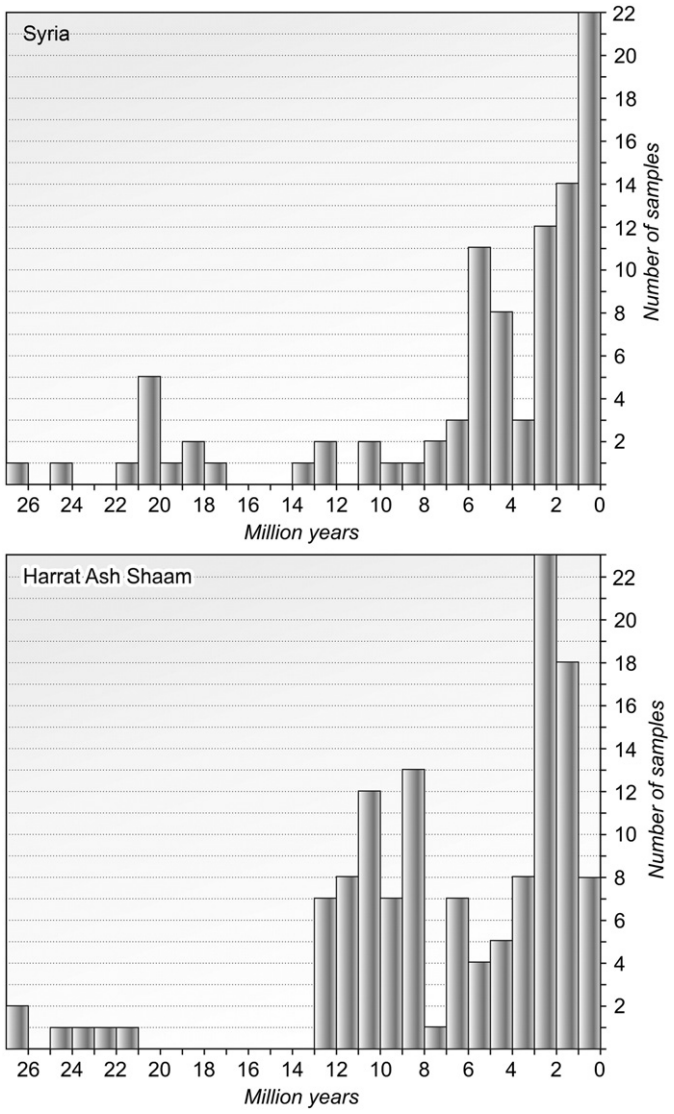

Fig. 6. Histogram of age distribution of the available K–Ar and Ar–Ar dates of the Syrian basalts, by the data in (Giannérini et al., 1988; Sharkov et al., 1994, 1998; Demir et al., 2007) and this paper, in comparison with analogous histogram for the Jordanian part of the Harrat Ash Shaam (Ilani et al., 2001). *N* is number of the dates.

same location in the northern margin of the Mesopotamian Foredeep between the upstreams of the Nahr El-Khabour River and the Tigris valley. The Pliocene and Quaternary basalts erupted close to the Euphrates valley. In the end of Pliocene, volcanism spread onto the recent DST zone, where centers of eruptions were located on the N-trending boundary and inner faults of pull-apart basins (Fig. 2 and Table 3).

The correlation between main stages of evolution of the basaltic volcanism and neotectonics demonstrates genetic links between these processes in the Arabian plate and its boundary zones and has to be taken into account for understanding volcanism origin.

6. On origin of Late Cenozoic basalts in Syria

A model of origin of the Late Cenozoic basaltic volcanism in Syria and the adjacent parts of the Arabian plate must account for the following peculiarities of that volcanism.

(1) Principal geochemical similarity of the basalts indicating mantle sources for the basalts (Stein and Hofmann, 1992).
(2) Volcanic areas are characterized by inherited development. The largest of them evolved for a long time, 26 million years in Jebel Arab–Harrat Ash Shaam and more than 15 million years in the Aleppo Plateau. Moreover, even some of individual volcanic chains (e.g., Jebel Arab) developed as inherited structures for several million years. There are no signs of one-way migration of volcanism. Such inheritance means that the magmatic sources moved together with the Arabian plate, and that magmatic sources were situated within the lithosphere mantle. This geological conclusion complies well with the results of geochemical studies of Weinstein (Segev, 2005) and Lustrino and Sharkov (2006).
(3) Although only a part of volcanoes and basaltic fields demonstrate direct links with individual crustal structures of the Arabian plate and its surrounding, there is the chronological coincidence between variations of intensity and distribution of volcanism and geodynamic changes and tectonic events along the Arabian plate boundaries. Volcanism was renewed in the former zones or occupied new areas in the favourable geodynamic situation. In the Shin area, decompression of the lithosphere, produced by the geodynamic situation caused changes in chemical composition of basalts and structural rebuilding of the northern DST zone.

We propose the following explanation of origin of the Syrian Cenozoic basalts that may account for all the peculiarities mentioned above. A portion of the northern drift of the Arabian lithosphere plate is caused by motion of the plate on the asthenosphere flow. The flow moved out of the Ethiopia–Afar superplume, which rose from the lower mantle (Ebinger and Sleep, 1998; Ershov and Nikishin, 2004). The flow eroded the Arabian plate deep interface, and magmatic sources were formed within decompressed sites of the lower lithosphere. As the potential of the sources was supported by the sub-lithosphere lateral flow, the sources produced basaltic eruptions at the same areas for a long time. At the same time, eruptions were only possible, when the geodynamic setting favoured initiation and activity of channels for magma passage. Dependence of volcanism on the geodynamic situation explains synchronism in the occurrence of volcanic activity and tectonic events within and near the Arabian plate. The local geodynamic changes in the Shin area led not only to the structural rebuilding in the northern DST zone, but caused the temporal geochemical changes in the composition of the erupted basalts. In Miocene, the sub-lithosphere flow penetrated into the inner zones of the Alpine–Himalayan collision belt up to the Great Caucasus and contributed to the Late Miocene–Quaternary volcanism there.

Composition of material involved in the sub-lithosphere flow changed in process of its northern movement due to partial crystallization and inclusions of the asthenosphere material. The lower lithosphere magmatic sources also included the local melted material. This is why the geochemical traces of the Ethiopia–Afar superplume have been found only in volcanic rocks in the southern part of the Arabian plate (Altherr et al., 1990; Baker et al., 1997; Bertrand et al., 2003). Northerly, as in Syria, basalts miss the superplume characteristics (Lustrino and Sharkov, 2006).

7. Conclusion

The Late Cenozoic basaltic volcanism began in Syria in the end of Oligocene (26–24 Ma). Over the Late Oligocene–Early Miocene time, it concentrated in the N-trending band, which stretched from the Jebel Arab–Harrat Ash Shaam to Kurd Dagh and the southern Turkey. Volcanic activity waned in the Middle Miocene (17–12 Ma), but resumed in the same band in the Tortonian and, with increased activity, in the Messinian and Early Pliocene (6.3–4 Ma), spreading into the Shin Plateau and its coastal continuation. After the ~4–3.5 Ma wane, volcanism became even more intensive in Jebel Arab and spread from the N-trending band both to the east, into the Euphrates

Valley and the northern margin of the Mesopotamian Foredeep, and to the west, into the DST zone. The eruptions went on in the Holocene.

The volcanism lasted for 26 million years in the Jebel Arab Highland and for >15 million years in the Aleppo Plateau. In the Jebel Arab Highland, long-time inheritance is characteristic not only for the volcanic area as a whole, but even for the individual linear zones of fissure eruptions. Long duration and inheritance of volcanism in the same areas of the moving Arabian plate as well as the absence of any signs of one-way migration of volcanism suggest that the magmatic sources were moving with the plate, and were situated within the lithosphere mantle. Synchronism of tectonic events in the plate boundary zones and periods of volcanic activity may be interpreted in such a way that volcanism (its intensity, distribution, sometimes even geochemical peculiarities, as in the Shin area) much depends on the geodynamic situation, primarily the plate motion. Situated in the lower lithosphere, the magmatic sources underwent deformational and thermal influence of the asthenosphere lateral flow that moved laterally from the Ethiopia–Afar deep superplume.

Acknowledgements

The studies were supported by the Program 6 “Geodynamics and physical processes in the lithosphere and upper mantle” of the Department of Geosciences of the RAS and the Project “Geodynamics of Syria” of the GORS, Syria.

References

Abdel-Rahman, A.-F.-M., Nassar, Ph.E., 2004. Cenozoic volcanism in the Middle East: petrogenesis of alkali basalts from northern Lebanon. Geol. Mag. 141, 545–563.

Alici, P., Temel, A., Gourgaud, A., Vidal, Ph., Nyazi Gundoglu, M., 2001. Quaternary tholeiitic to alkaline volcanism in the Karasu valley, Dead Sea rift zone, southeast Turkey: Sr–Nd–Pb–O isotopic and trace-element approaches to crust–mantle interaction. Intern. Geol. Rev. 43, 120–138.

Altherr, R., Henjes-Kunst, F., Baumann, A., 1990. Asthenosphere versus lithosphere as possible sources for basaltic magmas erupted during formation of the Red Sea: constraints from Sr, Pb and Nd isotopes. Earth Planet. Sci. Lett. 96, 269–286.

Ammar, O., 1993. Properties of the Geological Structure of the Southwestern Syria and Evaluation of the Ground Water Resources by Interpretation of Remote Sensing Data. Ph. D. Thesis, Moscow, 156 p. (in Russian).

Arger, J., Mitchell, J., Westaway, R., 2000. Neogene and Quaternary volcanism of southeastern Turkey. In: Bozkurt, E., Winchester, J.A., Piper, J.D.A. (Eds.), Tectonics and Magmatism in Turkey and the Surrounding Area: Geol. Soc. London Spec. Publ., 173, pp. 459–487.

Baker, J.A., Mensies, M.A., Thirlwall, M.F., MacPherson, C.G., 1997. Petrogenesis of Quaternary intraplate volcanism, Sana'a, Yemen: implications for plume–lithosphere interaction and polybaric melt hybridization. J. Petrol. 36, 1359–1390.

Barazangi, M., Seber, D., Chaimov, T., Best, J., Litak, R.D., Sawaf, T., 1993. Tectonic evolution of the northern Arabian plate in western Syria. In: Boschi, E., Mantovani, E., Morelli, A. (Eds.), Recent Evolution and Seismicity of the Mediterranean Region. Kluwer Acad. Publ., Dordrecht, pp. 117–140.

Barberi, F., Capaldi, G., Gasperini, P., Marinelli, G., Santacroce, R., Scandone, R., Treuil, M., Valet, J., 1979. Recent basaltic volcanism of Jordan and its implications on the geodynamic history of the Dead Sea shear zone. Acc. Naz. Lincei, Atti dei Convegni 47, 667–683.

Bertrand, H., Chazot, G., Blichert-Toft, J., Thoral, S., 2003. Implications of widespread high-μ volcanism on the Arabian Plate for Afar mantle plume and lithosphere composition. Chem. Geol. 198, 47–61.

Besançon, J., Sanlaville, P., 1981. Apercu geomorphologique sur la vallee de l'Euphrate Syrien. Paleorient 7 (2), 5–18.

Camp, V.E., Roobol, M.J., 1989. The Arabian continental alkali basalt province. Geol. Soc. Amer. Bull. 101, 71–95.

Camp, V.E., Roobol, M.J., 1992. Upwelling asthenosphere beneath western Arabia and its regional implication. J. Geophys. Res. 97, 15,255–15,271.

Çapan, U.Z., Vidal, Ph., Cantagrel, J.M., 1987. K–Ar, Nd, Sr and Pb isotopic study of Quaternary volcanism in Karasu Valley (Hatav), N-end of Dead-Sea Rift zone in SE Turkey. Verbilimleri 14, 165–178.

Chorowicz, J., Dhont, D., Ammar, O., Rukieh, M., Bilal, A., 2004. Tectonics of the Pliocene Homs basalts (Syria) and implications for the Dead Sea Fault Zone activity. J. Geol. Soc. London 161, 1–13.

Debayle, E., Leveque, J.-J., Cara, M., 2001. Seismic evidence for a deeply rooted low-velocity anomaly in the upper mantle beneath the northeastern Afro/Arabian continent. Earth Planet. Sci. Lett. 193, 423–436.

Demir, T., Westaway, R., Bridgland, D., Pringle, M., Yurtmen, S., Beck, A., Rowbotham, G., 2007. Ar–Ar dating of Late Cenozoic basaltic volcanism in northern Syria: implications for the history of incision by the River Euphrates and uplift of the northern Arabian Platform. Tectonics 26. doi:10.1029/2006TC001959 TC 3012.

Devyatkin, E.V., Dodonov, A.E., 2000. Stratigraphy of the Neogene and Quaternary deposits. In: Leonov, Yu.G. (Ed.), Outline of Geology of Syria. Nauka Press, Moscow, pp. 129–176.

Ebinger, C.J., Sleep, N.S., 1998. Cenozoic magmatism throughout east Africa resulting from impact of a single plume. Nature 395 (22), 788–791.

Ershov, A.V., Nikishin, A.M., 2004. Recent geodynamics of the Caucasus–Arabia–East Africa region. Geotectonics 38 (2), 123–136.

Ershov, A.V., Nikishin, A.M., Brune, M.-F., Spakman, V., 2001. Late Cenozoic geodynamics of the Caucasus region: data of numerical modeling and seismo-tomography. Tectonics of the Neogeic: General and Regional Aspects, vol. II. GEOS Publ., Moscow, pp. 230–235 (in Russian).

Garfunkel, Z., 1989. Tectonic setting of Phanerozoic magmatism in Israel. Isr. J. Earth Sci. 38, 51–74.

Garfunkel, Z., Ben-Abraham, Z., 2001. Basins along the Dead Sea Transform. In: Ziegler, P.A., Cavazza, W., Robertson, A.H.F., Crasquin-Soleau, S. (Eds.), Peri-Tethys Memoir 6: Peri-Tethyan Rift/Wrench Basins and Passive Margins: Memo ires du Muse um national d'Histoire naturelle, 186, pp. 607–627.

Geological Map of Syria. Scales 1:200 000 / Ponicarov, V. (Ed.) 1964. Technoexport, Moscow; Ministry of Industry of the S.A.R., Damascus.

Giannérini, G., Campredon, R., Feraud, G., Abou Zakhem, B., 1988. Deformations intraplaques et volcanisme associe: Exemple de la bordure NW da plaque Arabique au Cenozoique. Bull. Soc. Géol France (No. 6), 938–947.

Hurwitz, S., Garfunkel, Z., Ben-Gai, Y., Reznikov, M., Rotstein, Y., Gvirtzman, H., 2002. The tectonic framework of a complex pull-apart basin: seismic reflection observations in the Sea of Galilee, Dead Sea transform. Tectonophysics 359, 289–306.

Ilani, S., Harlavan, Y., Taravneh, K., Rabba, I., Weinberger, R., Ibraham, K., Peltz, S., Steinitz, G., 2001. New K–Ar ages of basalts from the Harrat Ash Shaam volcanic field in Jordan: implications for the span and duration of the upper-mantle upwelling beneath the western Arabian plate. Geology 29, 171–174.

Izzeldin, A.Y., 1987. Seismic, gravity and magnetic surveys in the central part of the Red Sea: their interpretation and implications for the structure and evolution of the Red Sea. Tectonophysics 143, 269–306.

Kaz'min, V.G., 1974. On certain specific features of riftogenesis (as exemplified by the evolution of the Red Sea, Aden and Ethiopian rifts). Geotectonics 8 (6), 3–14 (in Russian).

Kopp, M.L., Leonov, Yu.G., 2000. Tectonics. In: Leonov, Yu.G. (Ed.), Outline of Geology of Syria. Nauka Press, Moscow, pp. 7–104.

Krasheninnikov, V.A., 2005. Paleogene. Geological Framework of the Levant, Vol. I, Part 2. Historical Production-Hall, Jerusalem, pp. 299–342.

Lustrino, M., Sharkov, E., 2006. Neogene volcanic activity of western Syria and its relationship with Arabian plate kinematics. J. Geodyn. 42, 115–139.

Mouty, M., Delaloye, M., Fontignie, D., Piskin, O., Wagner, J.J., 1992. The volcanic activity in Syria and Lebanon between Jurassic and actual. Schweiz. Miner. Petr. Mitt. 72, 91–105.

Muhesen, S., 1985. L'Acheuleen Recent Evolue de Syrie. BAR Intern. Ser. 248, 1–189.

Polat, A., Kerrich, R., Casey, J.F., 1997. Geochemistry of Quaternary basalts erupted along the East Anatolian and Dead Sea fault zones of southern Turkey: implications for mantle sources. Lithos 40, 55–68.

Ponikarov, V.P., Kazmin, V.G., Mikhailov, I.A., Razvalyaev, A.V., Krasheninnikov, V.A., Kozlov, V.V., Soulidi-Kondratyev, E.D., Mikhailov, K.Ya., Kulakov, V.V., Faradjev, V.A., Mirzayev, K.M., 1967. Geological Map of Syria, Scale 1:500,000. Explanatory Notes. Part I. Ministry of Industry, Damascus, 230 p.

Rukieh, M., Trifonov, V.G., Dodonov, A.E., Minini, H., Ammar, O., Ivanova, T.P., Zaza, T., Yusef, A., Al-Shara, M., Jobaili, Y., 2005. Neotectonic map of Syria and some aspects of Late Cenozoic evolution of the north-western boundary zone of the Arabian plate. J. Geodyn. 40, 235–256.

Savostin, L.A., Sibuet, J.-C., Zonenshain, L.P., 1986. Kinematic evolution of the Tethys belt from the Atlantic Ocean to the Pamirs since the Triassic. Tectonophysics 123, 1–35.

Segev, A., 2005. Magmatic rocks. Geological Framework of the Levant, Vol. II, Part 4. Historical Production-Hall, Jerusalem, pp. 553–576.

Sharkov, E.V., 2000. Mesozoic and Cenozoic volcanism. In: Leonov, Yu.G. (Ed.), Outline of Geology of Syria. Nauka Press, Moscow, pp. 177–200.

Sharkov, E.V., Chernyshev, I.V., Devyatkin, E.V., Dodonov, A.E., Ivanenko, V.V., Karpenko, M.I., Leonov, Yu.G., Novikov, V.M., Hanna, S., Khatib, K., 1994. Geochronology of Late Cenozoic basalts in Western Syria. Petrology 2 (4), 385–394.

Sharkov, E.V., Snyder, G.A., Taylor, L.A., Laz'ko, E.E., Jerde, E., Hanna, S., 1996. Geochemical peculiarities of the asthenosphere beneath the Arabian plate: evidence from mantle xenoliths of the Quaternary Tell-Danun volcano (Syrian–Jordan plateau, southern Syria). Geochem. Int. 34, 737–752.

Sharkov, E.V., Chernyshev, I.V., Devyatkin, E.V., Dodonov, A.E., Ivanenko, V.V., Karpenko, M.I., Lebedev, V.A., Novikov, V.M., Hanna, S., Khatib, K., 1998. New data on the geochronology of Upper Cenozoic plateau basalts from northeastern periphery of the Red Sea rift area (Northern Syria). Doklady of Russian Academy of Sciences. Earth Sect. 358 (1), 19–22.

Shaw, J.E., Baker, J.A., Menzies, M.A., Thirlwall, M.F., Ibrahim, K.M., 2003. Petrogenesis of the largest intraplate volcanic field on the Arabian Plate (Jordan): a mixed lithosphere–asthenosphere source activated by lithospheric extension. J. Petrol. 44, 1657–1679.

Simkin, T., Siebert, L. (Eds.), 1994. Volcanoes of the World. A Regional Directory, Gazetteer, and Chronology of Volcanism During the Last 10,000 Years. Smithsonian Institution, Global Volcanism Program. Geoscience Press, INC., Tucson, Arizona. 349 pp.

Sobolev, S.V., Petrunin, A., Garfunkel, Z., Babeyko, A.Y., 2005. Thermo-mechanical model of the Dead Sea Transform. Earth Planet. Sci. Lett. 238, 78–95.

Stein, M., Hofmann, A.W., 1992. Fossil plume head beneath the Arabian lithosphere. Earth Planet. Sci. Lett. 114, 193–209.

Tatar, O., Piper, J.D.A., Gürsoy, H., Heimann, A., Koşbulut, F., 2004. Neotectonic deformation in the transition zone between the Dead Sea Transform and the East Anatolian Fault Zone, southern Turkey: a paleomagnetic study of the Karasu Rift volcanism. Tectonophysics 385, 17–43.

Trifonov, V.G., 1978. Problems of and mechanism for the tectonic spreading of Iceland. Modern Geol. 6 (3), 123–137.

Trifonov, V.G., 2007. The Bible and geology: destruction of Sodom and Gomorrah. Myth and Geology: Geol. Soc. of London. Special Publ., 273, pp. 133–142.

Trifonov, V.G., Karakhanian, A.S., 2008. Dynamics of the Earth and Development of the Society. OGI Press, Moscow. 436 pp. (in Russian).

Trifonov, V.G., Trubikhin, V.M., Adjamian, J., Jallad, Z., El Hair, Yu., Ayed, H., 1991. Levant fault zone in the north-western Syria. Geotectonics 25 (2), 145–154.

Weinstein, Y., Navon, O., Altherr, R., Stein, M., 2006. The role of lithospheric mantle heterogeneity in the generation of Plio-Pleistocene alkali basaltic suites from NW Harrat Ash Shaam (Israel). J. Petrol. 47, 1017–1050.

Yilmaz, V., Guner, Y., Saroglu, F., 1998. Geology of the Quaternary volcanic centers of the East Anatolia. J. Volcanol. Geotherm. Res. 85, 173–210.

Yürür, M.T., Chorowicz, J., 1998. Recent volcanism, tectonics and plate kinematics near the junction of the African, Arabian and Anatolian plates in the eastern Mediterranean. J. Volcan. Geothermal. Res. 85, 1–15.

Zanchi, A., Crosta, G.B., Darkal, A.N., 2002. Paleostress analyses in NW Syria: constraints on the Cenozoic evolution of the northwestern margin of the Arabian plate. Tectonophysics 357, 255–278.